Cellulose (2013) 20:771–783
DOI 10.1007/s10570-013-9870-1

ORIGINAL PAPER

Antimicrobial porous hybrids consisting of bacterial nanocellulose and silver nanoparticles

Sabrina Berndt · Falko Wesarg · Cornelia Wiegand · Dana Kralisch · Frank A. Müller

Received: 3 August 2012 / Accepted: 16 January 2013 / Published online: 26 January 2013

Abstract The increasing resistance of pathogens and bacteria is a serious problem in the medical treatment of wounds and injuries. Therefore, new therapeutic agents are not solely based on antibiotics, but also on the use of antimicrobial metal nanoparticles. In this paper we present an innovative method to prepare porous hybrids consisting of bacterial nanocellulose (BNC) and silver nanoparticles (AgNPs). The stepwise modification is based on fairly simple chemical reactions already described for two-dimensional cellulose films. We transferred this method to the three-dimensional, porous network of BNC leading to an antimicrobial activation of its surface. Compared to former approaches, the ultrafine network structure of BNC is less damaged by using mild chemicals. The amount and distribution of the AgNPs on the modified BNC was investigated using scanning electron microscopy. The AgNPs are firmly immobilized on the top and bottom surface of the BNC by chemical interactions. Their size and quantity increase with an increasing concentration of $AgNO_3$ and extended reaction time in the $AgNO_3$ solution. A strong antimicrobial activity of the BNC-AgNP hybrids against *Escherichia coli* was detected. Furthermore, agar diffusion tests confirmed that this activity is restricted to the modified dressing itself, avoiding a release of NPs into the wound. Therefore, the produced hybrids could be potentially suited as novel antimicrobial wound dressings.

Keywords Antimicrobial activity · Silver nanoparticles · *Escherichia coli* · Bacterial nanocellulose

S. Berndt and F. Wesarg contributed equally to this work.
D. Kralisch and F. A. Müller are members of the Jena Center for Soft Matter.

Electronic supplementary material The online version of this article (doi:10.1007/s10570-013-9870-1) contains supplementary material, which is available to authorized users.

S. Berndt · F. Wesarg · F. A. Müller
Institute of Materials Science and Technology (IMT), Friedrich-Schiller-University of Jena, Loebdergraben 32, 07743 Jena, Germany

C. Wiegand
Department of Dermatology and Allergology, University Medical Center Jena, Erfurter Strasse 35, 07743 Jena, Germany

D. Kralisch (✉)
Department of Pharmaceutical Technology, Institute of Pharmacy, Friedrich-Schiller-University of Jena, Otto-Schott-Strasse 41, 07745 Jena, Germany
e-mail: dana.kralisch@uni-jena.de

Introduction

The ancient Greeks, Egyptians, and Romans already used various metals and metal salts to clean wounds, taking advantage of their antimicrobial effect. However, the discovery of antibiotic substances has suppressed the utilization of antimicrobial metals in medical

applications. Today, clinicians face the serious problem of a growing number of pathogens having developed a resistance to antibiotics (Calfee 2012). Consequently, they intensively discuss the reuse of metals for wound-healing systems. Current research activities are mainly focused on the antimicrobial activity and effectiveness of silver nanoparticles (AgNPs) against various microorganisms (Schierholz et al. 1998; Monteiro et al. 2009; Zimmermann et al. 2011). It was demonstrated that AgNPs with their high specific surface area exhibit strong cytotoxicity towards fungi and viruses (Panyala et al. 2008; Monteiro et al. 2009). Furthermore, AgNPs lead to an enhanced growth inhibition of bacterial colonies such as *Staphylococcus aureus* and *Escherichia coli* (*E. coli*) (Sondi and Salopek-Sondi 2004; Cho et al. 2005). They can attach to the surface of the bacteria membrane and drastically disturb its proper function (e.g., permeability and respiration). Besides, the AgNPs are able to penetrate inside the bacteria and cause further damage by interacting with deoxyribonucleic acid (Morones et al. 2005). AgNPs usually release silver ions under physiological conditions. These silver ions accumulate on the functional (sulfhydryl-, phosphoryl-) groups of enzymes and proteins that are important for the metabolism of bacteria cells. Vital enzymes were inactivated, deoxyribonucleic acid loses its replication ability, and structural changes in the cell membrane occur. As a consequence, bacteria were inactivated as well (Sondi and Salopek-Sondi 2004; Morones et al. 2005; Gordon et al. 2010). Although the exact antimicrobial mechanism of AgNPs still remains unclear, it seems certain that several mechanisms lead to the inactivation of bacterial cells and impede the development of a resistance to silver (oligodynamic effect) (Knetsch and Koole 2011). However, a few studies pointed out occasional Ag-resistances of e.g. *Pseudomonas aeruginosa* (Bridges et al. 1979) or *E. coli* (Silver 2003) that may develop if the concentration of silver is not high enough to exert a bactericidal effect. Fortunately, the probability for the transfer of silver-resistance-genes seems to be low and difficult to maintain (Percival et al. 2005). Moreover, other studies have shown that bacteria carrying silver-resistant genes still remained susceptible to silver-dressings (Loh et al. 2009). Thus, the clinical threat can be considered low (Chopra 2007).

Consequently, nowadays a broad range of products making use of various scaffold materials and dressings for the immobilization of Ag and AgNPs is utilized in antimicrobial wound-healing systems (Castellano et al. 2007). Among them, bacterial nanocellulose (BNC) has recently attracted particular attention due to its outstanding properties. BNC is a highly biocompatible hydrogel that is produced by bacteria strains of the species *Gluconacetobacter xylinus* (Klemm et al. 2005; Klemm et al. 2011). It consists of a three-dimensional network of nanosized fibers (40–60 nm in diameter) with a high specific surface area (100–200 m^2/g) (Ishida et al. 2004; Klemm et al. 2006; Kralisch et al. 2010; Yun et al. 2010). It features a high purity, a high degree of polymerization (up to 8,000), a high crystallinity (up to 90 %), a high and controllable water content (approx. 99 %), and superior mechanical properties in the *never-dried* state (Klemm et al. 2001, 2005; Czaja et al. 2007; Kralisch et al. 2010). The high water absorption capacity and water retention allows to clean wounds, take up exudates and to sustain a humid and warm wound climate from which the healing process benefits significantly (Waring and Parsons 2001; Walker et al. 2003). Further, BNC represents an effective barrier to the entry of microorganisms (Fontana et al. 1990). Its suitability for the therapy of wounds, especially burns and ulcers, has been already demonstrated in several studies (Jonas and Farah 1998; Wiegand et al. 2006; Czaja et al. 2006, 2007; Solway et al. 2011). However, BNC itself does not feature an antimicrobial activity (Maneerung et al. 2008). This limitation can be overcome by developing hybrid materials which combine the antimicrobial properties of AgNPs with the unique structural properties of BNC. In recent years, various methods have been described to prepare such antimicrobial wound-healing systems (Maneerung et al. 2008; Sureshkumar et al. 2010; Barud et al. 2011; Yang et al. 2011, 2012). Most of them use $AgNO_3$ solutions in combination with strong reducing agents (e.g., sodium borohydride). However, the AgNPs tend to form relatively large particle agglomerates that are immobilized only by physical interactions and not by chemical bonds.

To avoid these disadvantages a more gentle modification of BNC was examined in this work. A stepwise modification was chosen, based on a procedure that was previously described for two-dimensional cellulose films (Alila et al. 2009; Ferraria et al. 2010). The method uses the grafting of diaminoalkanes that were activated by *N,N′*-carbonyldiimidazole (CDI). As a consequence, a CDI induced cross-linking of cellulose chains might occur. The possibility of this side-reaction was suggested in the context of dextran esterification (Heinze et al. 2006). However, the different phases of

the modification process were confirmed by Alila et al. (2009) and Ferraria et al. (2010) using cross-polarized/magic-angle spinning ^{13}C solid state nuclear magnetic resonance spectroscopy, fourier transform infrared (FT-IR) spectroscopy in attenuated total reflection in multiple internal reflections, X-ray photoelectron spectroscopy, as well as atomic force microscopy. In the experimental work of this group, dimethyl sulfoxide (DMSO) was used as a mild reducing agent. Appended amine groups operate as anchoring centers for the selective generation and chemical immobilization of the AgNPs (Boufi et al. 2011).

We transferred this method to three-dimensional, porous BNC substrates. The amount and distribution of the AgNPs immobilized on the BNC network were examined by scanning electron microscopy (SEM) equipped with energy dispersive x-ray analysis (EDX). The influence of parameters such as concentration of $AgNO_3$ and reaction time was determined. Furthermore, the antimicrobial activity of the BNC-AgNP hybrids was evaluated.

Materials and methods

Synthesis of BNC

BNC was synthesized by a static cultivation of the *Gluconacetobacter xylinus* strain DSM 14666 (German Collection of Microorganisms and Cell Cultures, Braunschweig, Germany) using the Hestrin-Schramm-Medium (HSM) as a culture medium (Hestrin and Schramm 1954). HSM was prepared by adding 10.0 g D-(+)-glucose (purity $\geq$ 99.5 %, Fluka, Buchs, Switzerland), 2.5 g bacto peptone (Difco Laboratories, Detroit, MI), 2.5 g yeast extract (Difco Laboratories, Detroit, MI), 1.7 g disodium hydrogen phosphate dihydrate (purity $\geq$ 99.5 %, Fluka, Buchs, Switzerland), and 0.575 g citric acid monohydrate (purity $\geq$ 99.5 %, Fluka, Buchs, Switzerland) to 500 mL of deionized water. The culture medium was adjusted to a pH-value of 6.0–6.3. Subsequently, it was sterilized by autoclaving at 121 °C for 20 min (VARIOKLAV, HP Medizintechnik, Oberschleißheim, Germany). 5 mL of the culture medium was pipetted in each well of a 12-well plate. A seven day old preparatory culture of the strain DSM 14666 was added to the culture medium in the ratio 1:20. The solution was cultivated under static conditions in an incubator (Binder, Tuttlingen, Germany) for 14 days at 28 °C. The resulting BNC fleeces were washed with distilled water and soaked in a boiling 0.1 N aqueous sodium hydroxide solution for 30 min. This method results in the removal of bacterial cells and components of the culture medium and therefore leads to a distinct decline of any amino compounds (Klemm et al. 2001; Wiegand et al. 2006). Subsequently, they were washed in distilled water until reaching a pH-value of approximately 7.0. Finally, the BNC-samples were sterilized by autoclaving at 121 °C for 20 min.

Preparation of BNC-AgNP hybrids

The modification of BNC with AgNPs was achieved by a three step procedure (Fig. 1). At first, BNC was activated in a solution of CDI ($c = 5.0 \times 10^{-2}$ mol/L) in anhydrous dimethyl sulfoxide (DMSO). 12 BNC-samples (dry mass 0.53 g) were immersed in a solution of 300 mL DMSO (purity > 99 %, $H_2O < 0.2$ %, Merck, Darmstadt, Germany) and 2.44 g CDI (Sigma-Aldrich, Munich, Germany) at 50 °C for 2 h while continuously stirred (Fig. 1a). Secondly, the BNC-samples were dipped into a solution of 1,4-diaminobutane (DAB, $c = 1.0 \times 10^{-2}$ mol/L) in anhydrous DMSO. For this purpose a solution consisting of 300 mL DMSO and 0.3 mL DAB (purity > 98 %, Alfa-Aesar, Karlsruhe, Germany) was prepared. The 12 activated BNC-samples were transferred directly from the CDI solution into this solution and were treated for 2 h at room temperature while continuously stirred (Fig. 1b). Subsequently, the BNC-samples were rinsed in 300 mL ethanol (purity $\geq$ 99.8 % with about 1 % methyl ethyl ketone, Roth, Karlsruhe, Germany) and then in 300 mL deionized water for 15 min using a magnetic stirrer in order to remove amines that are not chemically bound. In the last step, the BNC-samples were immersed in approximately 300 mL solution consisting of 150 mL DMSO, 150 mL deionized water, 0.02 g anhydrous sodium acetate (J.T. Baker, Deventer, Netherlands), and silver nitrate ($AgNO_3$, Applichem, Darmstadt, Germany) for 1 h at room temperature under continuous stirring (Fig. 1c). Finally, the modified BNC-samples were washed abundantly in deionized water. To evaluate the influence of the $AgNO_3$ concentration on the amount of incorporated AgNPs, $AgNO_3$ concentrations of 2.5×10^{-3} mol/L (Ag2.5), 5×10^{-3} mol/L (Ag5), 1×10^{-2} mol/L (Ag10), and 2×10^{-2} mol/L (Ag20) were used in the third modification step

(Fig. 1c). To evaluate the influence of the reaction time on the amount of incorporated AgNPs, the BNC-samples were immersed in a solution with a $AgNO_3$ concentration of 5×10^{-3} mol/L for 1 h (Ag5-1 h, correlates to Ag5), 2 h (Ag5-2 h), and 3 h (Ag5-3 h). Unmodified BNC-samples (BNC) were used as a reference. One half of the samples was *freeze-dried* at a pressure of 47 Pa and at a condenser temperature of −85 °C for 48 h (Christ Alpha 2-4 LSC, Osterode am Harz, Germany). The other half was sterilized by autoclaving at 121 °C for 20 min and stored in distilled water (*never-dried*).

Characterization of BNC-AgNP hybrids

Evidence for the occurrence of the reaction at each modification step was confirmed by FT-IR spectroscopy. *Freeze-dried* samples were directly measured using the attenuated total reflectance technique (Bruker Optics ALPHA FT-IR spectrometer, Bruker Optik, Ettlingen, Germany) with an accuracy of 4 cm^{-1}. All spectra were obtained by accumulation of 24 scans at 400–4,000 cm^{-1} and subsequent normalization at the band at 3,347 cm^{-1} due to the intramolecular hydrogen bonds of BNC. Analyses of the Water Absorption Capacity and Water Holding Capacity confirmed that no swelling or shrinking of the BNC material occurred due to the modification (see ESM 1). Additionally, elemental analyses of *freeze-dried* samples were performed using the mean value of 3 samples to detect nitrogen that could be introduced during the modification steps (Leco CHNS-932, LECO Instrumente GmbH, Mönchengladbach, Germany).

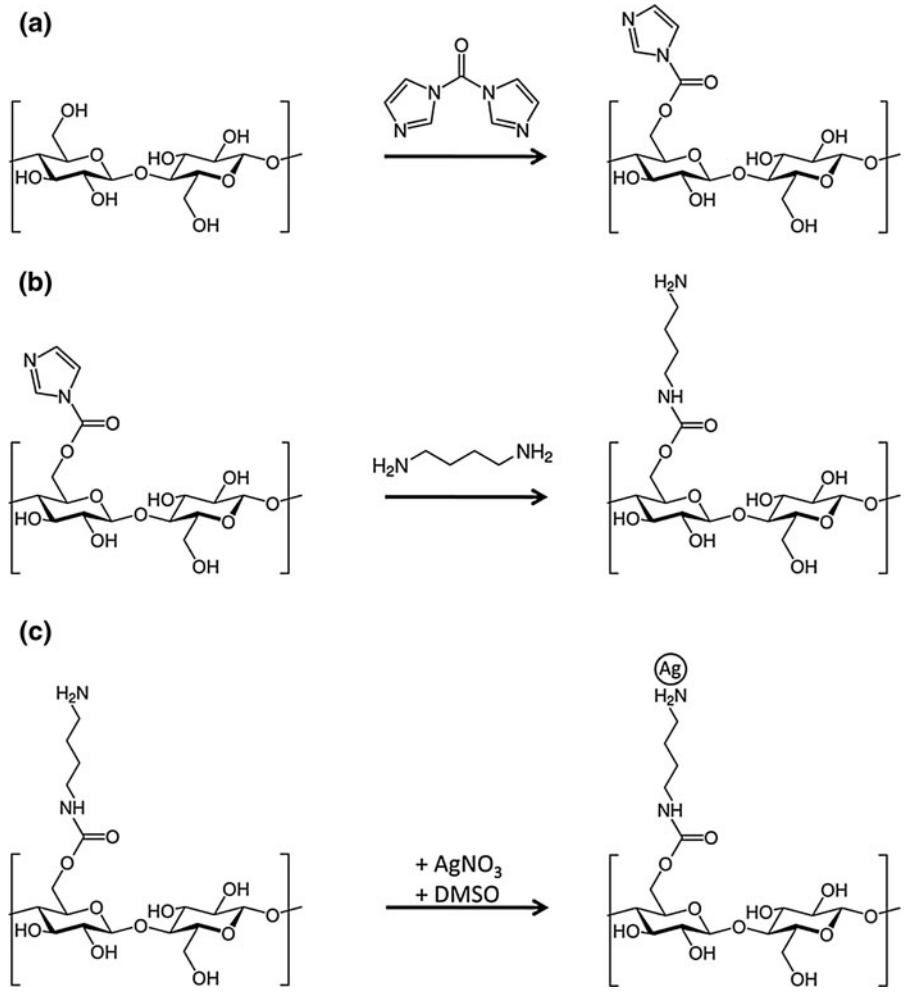

Fig. 1 Schematic illustration of the three step procedure to prepare hybrids consisting of BNC and AgNPs

The microstructure of the BNC-AgNP hybrids was examined by SEM (Leica S 440i, Wetzlar, Germany). *Freeze-dried* samples were sputtered with gold (Edwards Sputter Coater S150B, Crawley, UK). The top and bottom surface of the samples were examined both due to the anisotropic structure of BNC (Klemm et al. 2001; Wesarg et al. 2012). The amount and the distribution of the AgNPs of each $AgNO_3$ concentration and reaction time were determined from three SEM images. The digital image data were processed and evaluated using the software package ImageJ 1.45 (Wayne Rasband, Bethesda, MD). EDX analyses were carried out to verify the presence of silver by using the software Link Isis (Oxford Intruments, Oxfordshire, UK).

The antimicrobial activity of the top and bottom surface of three *never-dried* samples prepared at an $AgNO_3$ concentration of $c = 5.0 \times 10^{-3}$ mol/L and a reaction time of 1 h (Ag5) was evaluated by the BacTiter-GLO test (BTG test), the determination of colony forming units (CFU), and by agar diffusions tests. Pure BNC (BNC) was used as a reference. In the case of the BTG test and the CFU determination, the samples were transferred in 12-well plates with the surface facing upwards. *E. coli* bacteria from the strain HB 101 were cultivated in soybean casein digest medium (Sifin, Tryptic Soy Broth medium A, Berlin, Germany) (Zimmermann et al. 2011). Each sample was loaded with 1.0 mL *E. coli* suspension. Then the samples were placed in an incubator (GFL, Burgwedel, Germany) for 3 h at 37 °C and 90 rpm. The BTG test (Promega, Madison, USA) was used to detect the presence of bacteria. For testing, adenosine triphosphate (ATP) produced by living cells was utilized. The BTG reagent lyses the cells and converts the ATP by a luciferin-luciferase process which results in a luminescence signal (Zimmermann et al. 2011; Arora and Mitragotri 2010). 50 µL suspension from all cultured samples were transferred to a white non-transparent 96-well plate. 50 µL BTG reagent was added and mixed with a mixmate microplate shaker (Eppendorf, Hamburg, Germany) for 5 min at 850 rpm. The luminescence of the suspensions was measured in a microplate reader (Tecan, Genios Pro, Crailsheim, Germany). The initial luminescence of 1.0 mL *E. coli* suspension amounts to 75,000 counts. The results were analyzed by using the Magellan V 5.00 software. Furthermore, the antimicrobial effect was quantified by measuring the CFU of *E. coli* in the suspensions after contact with the samples. For this purpose, serial dilutions of each tested suspension were prepared and cultivated on agar plates. The agar plates were produced using soybean casein digest ager (Sifin, Tryptic Soy Agar, Berlin, Germany) as culture medium. Next, 100 µL suspension from each cultured sample were transferred and diluted 1-fold, 10-fold, 100-fold and 1,000-fold. 30 µL (inoculum) of each dilution were dripped on quartered agar plates. The agar plates were cultivated in an incubator at 37 °C for 18 h. Subsequently, the agar plates were scanned and the colonies that formed from a 1,000-fold dilution were counted. The number of CFU per milliliter suspension was calculated from the number of colonies, the level of dilution, and the inoculum (Bast 2001; Zimmermann et al. 2011).

Agar diffusion tests were used to evaluate the formation of an inhibition zone around the BNC-AgNP hybrids (Hipler et al. 2006). For this purpose, colonies of a pure culture of *E. coli* bacteria (DSM 5923, German Collection of Microorganisms and Cell Cultures, Braunschweig, Germany) were inoculated in 5 mL Mueller–Hinton broth (BD, Franklin Lakes, NJ) and incubated at 37 °C until the turbidity of the suspension was equal to that of 0.5 McFarland. The *E. coli* suspension was diluted 10-fold with physiologic saline solution (0.9 % NaCl) working in a class II biological safety cabinet (Thermo Scientific MSC-Advantage, Thermo Scientific, Waltham, MA). 100 µL inoculum was pipetted on a Mueller–Hinton 2 agar plate (bioMérieux Deutschland GmbH, Nürtingen, Germany). The suspension was evenly spread over the complete agar surface using a sterilized Drigalski spatula. After incubation for 15 min at room temperature, a drained sample was placed directly onto the surface of a germ-containing agar plate. Additionally, a positive control (amoxycillin/clavulanic acid) and a negative control (paper disc) were considered (Antimicrobial Susceptibility Test Discs, Oxoid Deutschland GmbH, Wesel, Germany). Then the agar plates were placed in an incubator (Memmert, Schwabach, Germany) for 24 h at 37 °C. After incubation, photographs were taken and the diameter of the inhibition zone surrounding the samples was measured.

Results and discussion

Formation of BNC-AgNP hybrids: Influence of the $AgNO_3$ concentration

The BNC-AgNP hybrids were prepared by a stepwise chemical modification (Fig. 1a, b, c). Figure 2 shows

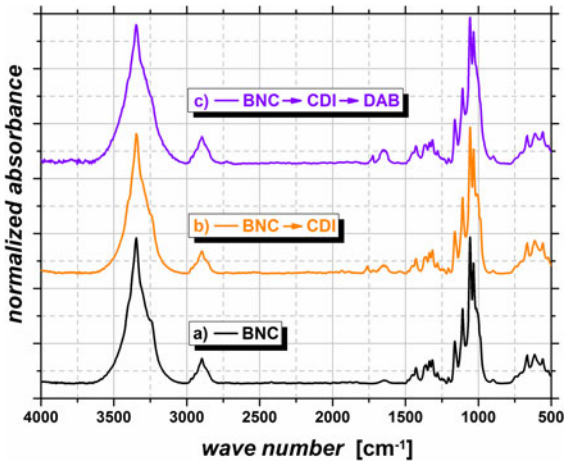

Fig. 2 FT-IR spectra of pure BNC (BNC) **a** before activation and after **b** activation with CDI, and **c** functionalization with DAB

the FT-IR spectra before (BNC) and after different stages of BNC treatment. The typical peaks for untreated BNC can be found at 3,347, 3,240, 2,896, 1,428, 1,163, 1,109, 1,058, 1,034 cm^{-1} (Fig. 2a) (Klemm et al. 2001; Wiegand et al. 2006; Alila et al. 2009). The activation of BNC with CDI resulted in the generation of imidazole ester derivatives (Fig. 1a) (Alila et al. 2009; Ferraria et al. 2010; Boufi et al. 2011). The spectral signature of cellulose remained unchanged. Besides, two additional peaks centered around 1,760 cm^{-1} assigned to the C=O stretching mode of the imidazole ester, and around 1,650 cm^{-1} assigned to C=C and C=N stretching modes of the imidazole heterocycle were obtained (Fig. 2b). A cross-linking of the cellulose chains induced by CDI can be excluded due to the absence of a carbonate peak centered around 1,430 cm^{-1}. Furthermore, the nitrogen content of the samples was investigated by elemental analyses. It was found to exceed that one of unmodified BNC (Table 1). During the second step of modification, imidazole ester derivatives facilitate the grafting of aliphatic amines through carbamate linkages (Fig. 1b) (Alila et al. 2009). Thus, the disappearance of these two bands was accompanied by the appearance of 2 new peaks. They correspond to NH asymmetric deformation (1,650 cm^{-1}) and C = O stretching vibrations (1,730 cm^{-1}) of the carbamate (Fig. 2c). The appearance of both peaks as well as the maintenance of an increased nitrogen content obtained during elemental analyses compared to unmodified BNC evidence the replacement of imidazole by a diaminobutyl group (Table 1). The slight discrepancy between the nitrogen content after first and second step of modification can be probably explained by uncertainties of measurement and the fact that different samples has to be used for determination.

The nucleation of silver was induced by silver ions that link to the diamines on the pretreated cellulose as described by Ferraria et al. (2010) and Boufi et al. (2011). These ions could be reduced to Ag^0 by DMSO (Rodríguez-Gattorno et al. 2002). Consequently, the growth of the AgNPs occurred selectively on the modified BNC by chemical interactions (Fig. 1c). The hybrids showed a slight gray color after this treatment. Furthermore, SEM micrographs that were taken at a higher magnification indicated the existence of nanoparticles on the top (ESM 4 c, e, g, and i) and bottom surface (ESM 4 d, f, h, and j) of the BNC-AgNP hybrids. However, SEM images that were taken at a lower magnification show aggregates of submicron dimensions and some larger aggregates on both surfaces (Fig. 3). The results of the EDX analyses manifested the presence of AgNPs with peaks located at $E_{L\alpha 1} = 2.984$ keV and $E_{L\beta 1} = 3.151$ keV (see Online Resource ESM 2) (Yang et al. 2012). In addition, a rising content of AgNPs was indicated with increased concentration of $AgNO_3$ (Fig. 3). The BNC-AgNP hybrids which were produced using the lowest concentration of $AgNO_3$ (Ag2.5) exhibited only a very small surface area of about 0.7 % occupied by silver particles (see Online Resource ESM 3, and Table 2). With rising concentration of $AgNO_3$ a relatively steady increase of the surface area occupied by AgNPs could be determined (see Online Resource ESM 3, and Table 2). A strikingly high amount of AgNPs was noticeable on the bottom surface of Ag20 (Fig. 3j and

Table 1 Results of elemental analyses of pure BNC and after treatment with CDI and DAB (Fig. 1)

	C (%)	H (%)	N (%)
BNC	43.47 ± 0.07	6.32 ± 0.05	0.10 ± 0.10
BNC → CDI	42.64 ± 0.02	6.21 ± 0.01	0.40 ± 0.07
BNC → CDI → DAB	42.83 ± 0.07	6.32 ± 0.07	0.29 ± 0.07

Online Resource ESM 3j) which was prepared at the highest concentration of $AgNO_3$ ($c = 2.0 \times 10^{-2}$ mol/l). Probably, the anisotropic structure of BNC only affects the amount of AgNPs at higher concentrations of $AgNO_3$. However, for all samples the amount of AgNPs increased with an increasing concentration of $AgNO_3$. This effect can also be explained by the growth of AgNPs that results in the formation of particle agglomerates (Fig. 3 and Online Resource ESM 3). Particle agglomerates were formed by clustering of individual AgNPs. In consequence, BNC-AgNP hybrids synthesized at low concentrations of $AgNO_3$ (Ag2.5 and Ag5) exhibit fine and very homogeneously distributed particle agglomerates compared to hybrids prepared at higher concentrations of $AgNO_3$ (Fig. 3). In this context, T. Maneerung et al. (2008) already observed that the molar ratio of the reducing agent (in their study $NaBH_4$) to $AgNO_3$ influenced the particle size distribution. By decreasing the ratio of the reducing agent to $AgNO_3$ an increase in particles size distribution of AgNPs was found. This implies for our work that the probability of agglomerate formation increases when the DMSO:$AgNO_3$ molar ratio is decreased. An excess of silver ions in solution led to a more pronounced aggregation (Ag10 and Ag20). Similar observations were also reported in literature (Maneerung et al. 2008; Barud et al. 2011). Freshly reduced AgNPs formed aggregates with silver that already adsorbed on the cellulose fibers. The aggregation process did not cease until all metal ions in solutions were consumed, resulting in larger particles on BNC at higher concentrations of $AgNO_3$. In contrast, a narrow size distribution was found when the DMSO:$AgNO_3$ molar ratio was increased (Ag2.5 and Ag5). This is probably due to the amount of free electrons generated from DMSO which was high enough to prevent the aggregation of silver (Maneerung et al. 2008). The results of SEM investigations support this theory (Online Resource ESM 3). In summary, the size distribution of AgNPs can be easily controlled by adjusting the molar ratio of DMSO to $AgNO_3$. The hybrid Ag5 was prepared at a concentration of $AgNO_3$ of $c = 5.0 \times 10^{-3}$ mol/L, using the same concentration as proposed by (Ferraria et al. 2010). However, the AgNPs form agglomerates at the top (Online Resource ESM 3e) and the bottom surface (Online Resource ESM 3f) up to approximately 1 μm in size which differs from the observations made by Ferraria et al. This mismatch might be caused by the hydrogel character of BNC, supporting the growth of AgNPs. The AgNPs cluster to larger agglomerates at those points where the modification started. This explanation is equally applicable to an increasing ratio of reducing agent to $AgNO_3$. The hydrogel character of BNC further limits the accessibility of the hydroxyl groups. Consequently, the different fibrous structures of the top surface and the bottom surface do not affect the silver content significantly. Another relevant difference between both investigations is the circumstance that the first reaction steps were not carried out under complete anhydrous conditions due to the high water content of BNC (Klemm et al. 2005). In fact, the AgNPs were selectively and directly generated on *never-dried* BNC fibers due to grafted amino groups acting as nucleating sites, without any growth of AgNPs in the reaction solution. Beyond that, the BNC-AgNP hybrids kept their grey color after a 5 times repeated solvent exchange by deionized water. That indicates firmly immobilized AgNPs on BNC as described by Ferraria et al. (2010) for cellulose films. In opposition to other methods applied to BNC, the AgNPs are chemically linked to the BNC carrier. As an example, Sureshkumar et al. (2010) reported that AgNPs impregnated BNC hybrid that was prepared by immersing modified BNC in $AgNO_3$ solution, showed a decreased antimicrobial efficiency after 6 repeated uses. The decrease was caused by the AgNPs leakage during incubation in bacterial solution and restricted its applicability. On the contrary, the application of the proposed method allows the preparation of innovative hybrids consisting of BNC and AgNPs that show enhanced lifetimes.

Formation of BNC-AgNP hybrids: Influence of the reaction time

In order to determine the influence of the reaction time in the $AgNO_3$ solution on the resulting surface area covered by AgNPs, BNC was modified with a concentration of $AgNO_3$ of $c = 5.0 \times 10^{-3}$ mol/L (Ag5) and different exposure times (1–3 h). A clear correlation between the reaction time and the amount of AgNPs on the top (Fig. 4a, c, and e; Online Resource ESM 4a, c, and e) and bottom surface (Fig. 4b, d, and f; Online Resource ESM 4b, d, and f) of the hybrids was detected. Starting from the standard reaction time (Ag5-1 h), the amount of AgNPs increased from about 3.5 % up to 20 % for the Ag5-

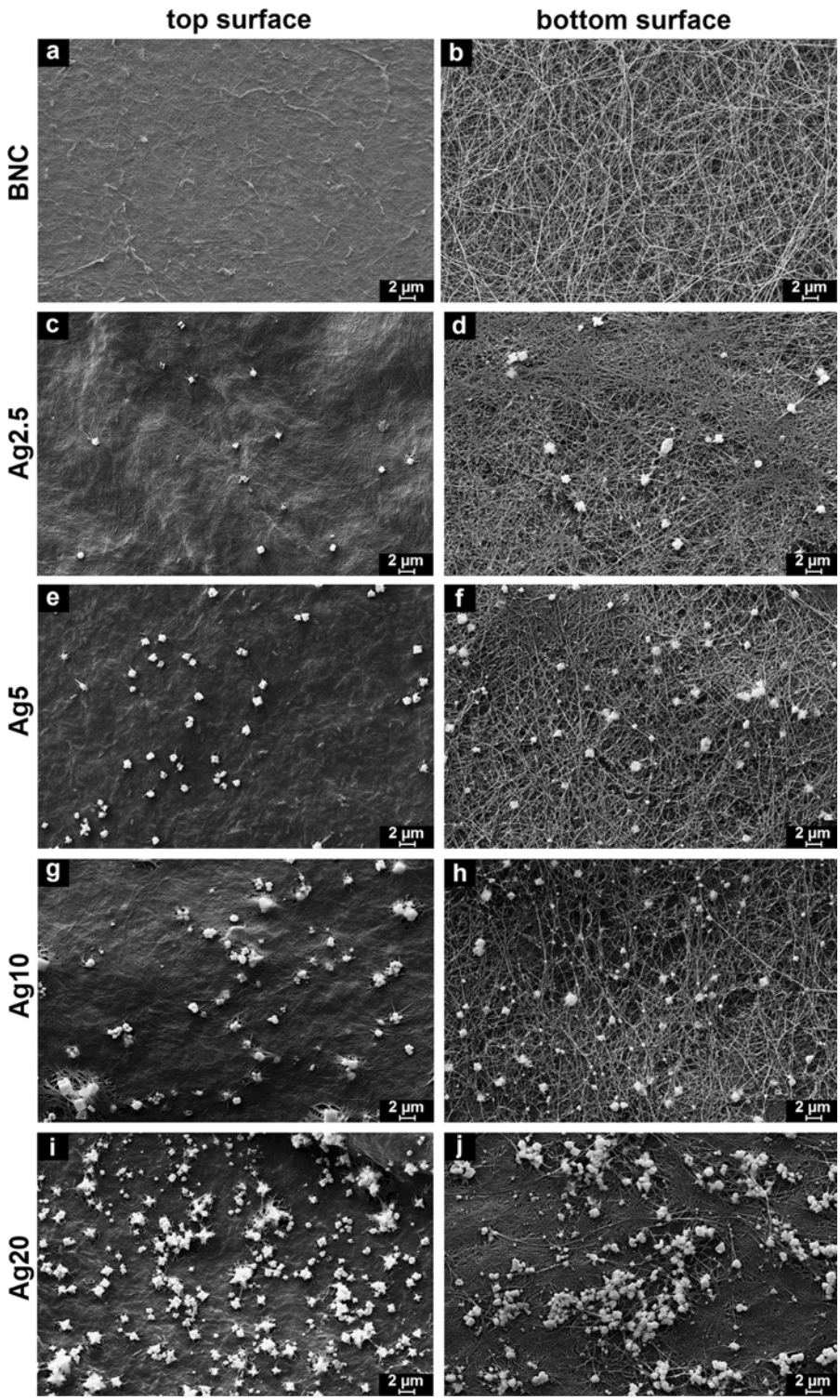

Fig. 3 SEM micrographs of BNC-AgNP hybrids taken from the *top* (**a**, **c**, **e**, **g** and **i**) and *bottom* surface (**b**, **d**, **f**, **h** and **j**)

Table 2 Average surface ratio of silver on the top and bottom surface of BNC-AgNP hybrids

	BNC	Ag2.5	Ag5	Ag10	Ag20
Top surface (%)	0	0.7 ± 0.3	3.2 ± 1.4	5.6 ± 0.5	7.0 ± 2.4
Bottom surface (%)	0	0.6 ± 0.4	3.7 ± 1.0	4.2 ± 1.2	11.8 ± 2.3

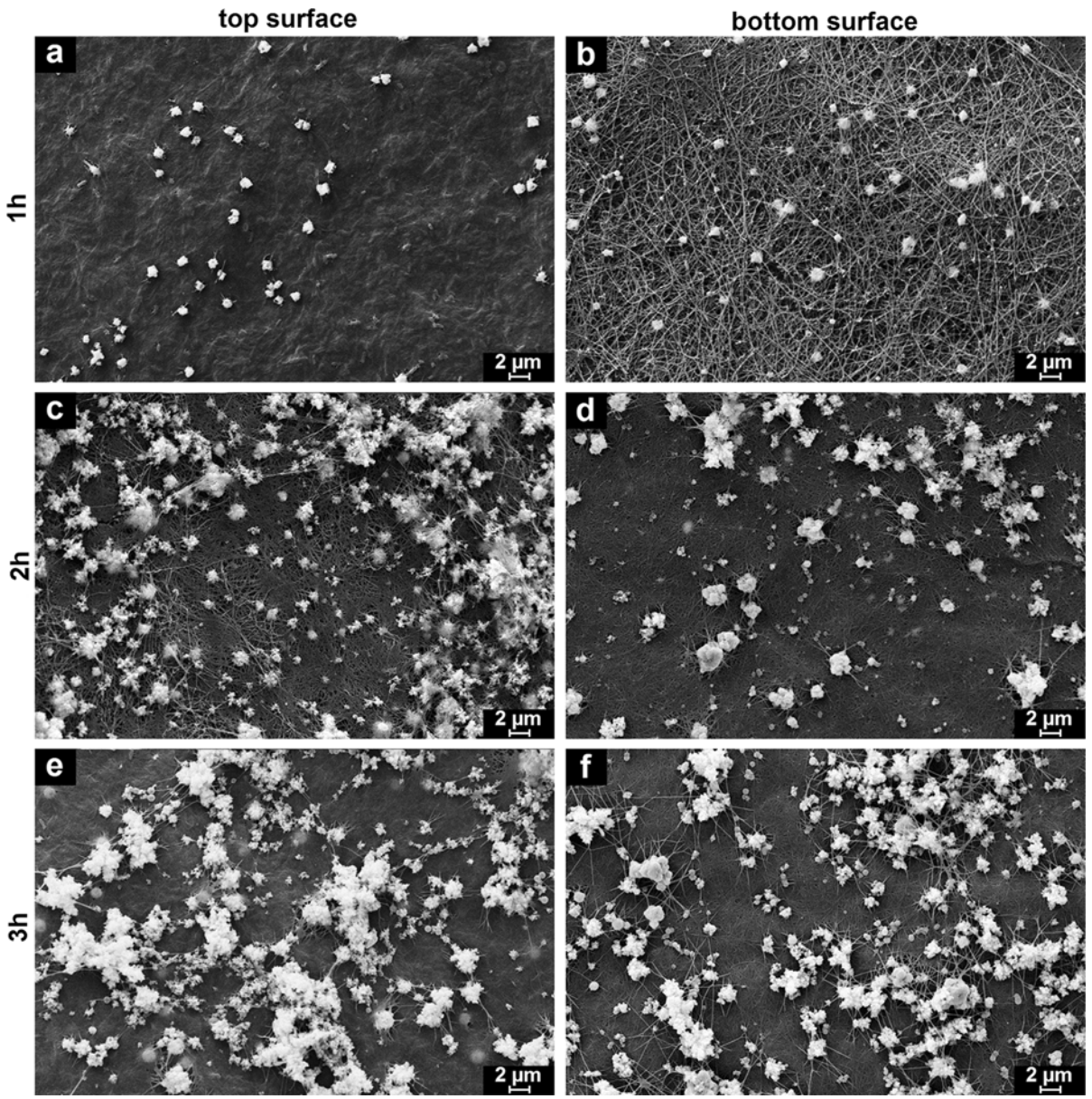

Fig. 4 SEM micrographs of Ag5 hybrids prepared for different reaction times. The micrographs were taken from the *top* (**a**, **c** and **e**) and *bottom* surface (**b**, **d**, and **f**)

Table 3 Average surface ratio of silver on the top and bottom surface of Ag5 hybrids prepared for different reaction times

	1 h (Ag5-1 h)	2 h (Ag5-2 h)	3 h (Ag5-3 h)
Top surface (%)	3.2 ± 1.4	11.8 ± 4.7	17.2 ± 4.0
Bottom surface (%)	3.7 ± 1.0	13.1 ± 4.1	20.6 ± 3.6

3 h hybrid that was exposed to $AgNO_3$ for 3 h (Table 3). The surface area covered by AgNPs on the top and bottom surface was found to be comparably high. In addition, a significant increase of the size of agglomerates up to approximately 5 µm was found with increasing exposure time in the $AgNO_3$ solution (Online Resource ESM 4). This effect led to an increase of the AgNPs content. Only freely accessible hydroxyl groups were modified in the activation process. Thus, selective growth of AgNPs could only take place on these sites. Over time, more and more AgNPs grew together and formed clusters. Finally large agglomerates were obtained.

Antimicrobial activity of BNC-AgNP hybrids

Colony forming units (CFU) obtained by the cultivation of *E. coli* suspensions on agar plates were used to evaluate the antimicrobial activity of the BNC-AgNP hybrids. Hybrids prepared with a concentration of $AgNO_3$ of $c = 5.0 \times 10^{-3}$ mol/L (Ag5) were chosen for this test, whereas pure BNC (BNC) served as a reference. On the top (Fig. 5a) and on the bottom surface (Fig. 5c) of BNC, the number of CFU amounts to 22 and 24 at highest dilution, respectively. Thus, approximately 7×10^5 CFU per mL were found on unmodified BNC (Table 4). In contrast, not any colony forming unit was present on the top (Fig. 5b) or on the bottom surface (Fig. 5d) of Ag5 hybrids (0 CFU per mL). The hybrids inactivated all bacteria that were able to proliferate. Generally, a low antimicrobial activity is defined to be less than a 1-log reduction, a moderate activity is characterized by a 1-and 3-log reduction, and a high antimicrobial activity is given at a 3-log reduction and more (Gallant-Behm et al. 2005). Thus, the 5-log reduction of bacteria found for the Ag5 hybrids confirmed a high antimicrobial activity of the BNC-AgNP hybrids already accessible at low concentrations of $AgNO_3$. The antimicrobial activity of the top and bottom surface of the Ag5 hybrids was found to be roughly the same. This correlates with the comparable amount and distribution of AgNPs on the top and bottom surface of these samples. The results of the CFU tests were confirmed by the BTG test. Figure 6 shows that the number of living bacteria was significantly reduced by the Ag5 hybrids (low luminescence) compared to pure BNC (high luminescence). The initial luminescence of 1.0 mL *E. coli* suspension amounted to 75,000 counts. BNC showed approximately 110,000 counts on the top and about 90,000 counts on the bottom surface, respectively (Fig. 6 and Table 4). As a result, it can be stated that the bacteria multiplied on pure BNC. In contrast, the decrease of the luminescence amounts to 1,300 counts on the top surface and to 500 counts on the bottom surface of Ag5 hybrids. Thus, the bacterial population was reduced by approximately 99 % compared to pure BNC. The luminescence of top surfaces was significantly higher than that one of bottom surfaces. However, it should be noted that the examined surfaces of all tested samples was facing upward. This could have led to an attenuation of the luminescence signal due to a stronger subsidence of bacteria on the bottom surface of the BNC during luminescence measurement. Furthermore, the distinction could be explained by the slightly lower

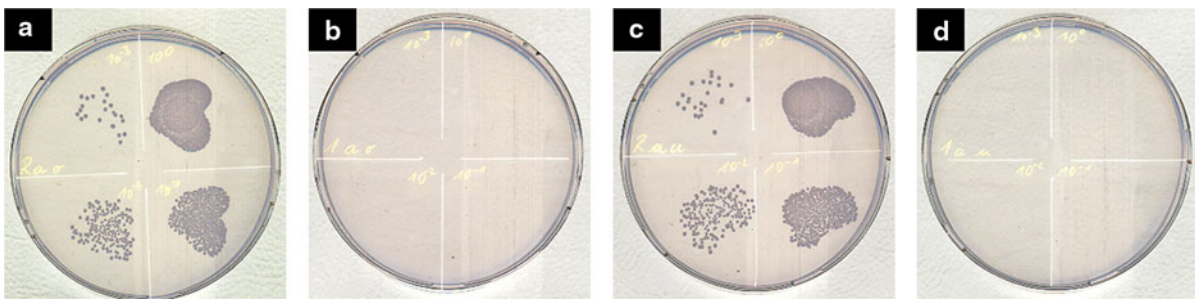

Fig. 5 CFU test of serial dilutions from *E. coli* suspensions after contact to **a** the *top surface* of pure BNC (BNC), **b** the *top surface* of Ag5 hybrids, **c** the *bottom* surface of pure BNC (BNC), and **d** the *bottom surface* of Ag5 hybrids

Table 4 Number of colonies on pure BNC (BNC) and on the hybrid Ag5 at highest dilution, corresponding CFU values as well as their average luminescence during BTG test

	Colonies	CFU (1/mL)	Luminescence (counts)
Top surface BNC	24 ± 1	783,333 ± 23,570	110,091 ± 7,462
Top surface Ag5	0	0	1,293 ± 193
Bottom surface BNC	22 ± 4	733,333 ± 141,421	89,955 ± 10,078
Bottom surface Ag5	0	0	515 ± 107

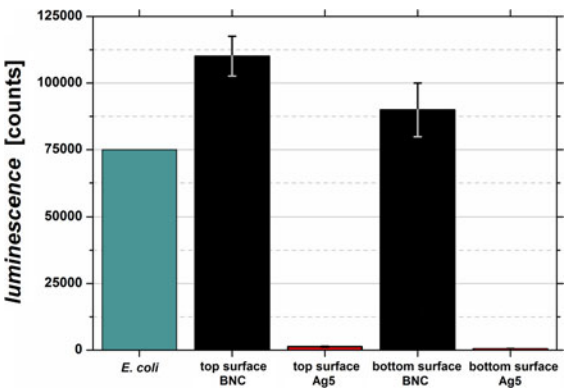

Fig. 6 Average luminescence of the *top* and *bottom surfaces* of pure BNC (BNC) and Ag5 hybrids. Values were derived from BTG tests with a 1 mL *E. coli* suspension serving as a reference

AgNPs content on the top surfaces (3.2 %) of the Ag5 hybrids compared to the corresponding bottom surfaces (3.7 %). The results of the BTG tests were consistent to those of the CFU tests. However, the antimicrobial activity measured by BTG tests was less pronounced due to a residual background noise of the luminescence signal (Zimmermann et al. 2011).

The results of agar diffusion tests are shown in Fig. 7. Pure BNC (Fig. 7a, c), the BNC-AgNP hybrid Ag5 (Fig. 7b, d), and the negative controls were characterized by the absence of an inhibition zone after incubation for 24 h. The bacteria around the hybrids were not affected. This result was independent from the tested surface side. The positive controls exposed inhibition zones with diameters of about 19–20 mm. Consequently, the AgNPs that are immobilized on the hybrid surface operate as an antimicrobial agent only in direct contact with bacteria. Due to the remaining risk of silver resistances induced by released silver ions into the wound, this effect might become an advantage against alternative silver containing wound dressings.

However, the agar diffusion tests were not performed in a moist milieu. A higher humidity may accelerate the release of silver ions during the tests. Furthermore, a prolonged incubation time or a higher content of AgNPs (e.g., Ag10 and Ag20) could trigger the release of silver ions. This aspect will be investigated in detail in further studies. The results of the agar diffusion test also confirmed that no imidazole residues are present in the final BNC-AgNP hybrids. It is known that numerous imidazole derivatives show active antimicrobial effects (Bhanat et al. 2011; Chawla et al. 2012) that would have caused the formation of an inhibition zone during agar diffusions test.

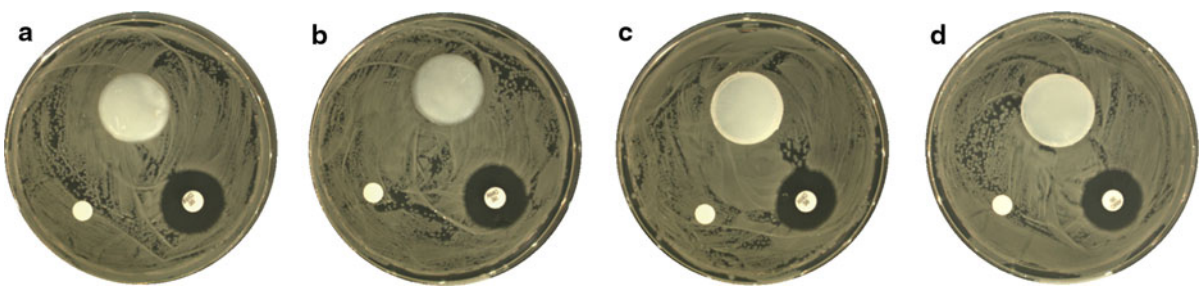

Fig. 7 Results obtained from agar diffusion tests of **a** the *top surface* of pure BNC, **b** the *top* surface of Ag5 hybrids, **c** the *bottom surface* of pure BNC, and **d** the *bottom surface* of Ag5 hybrids; **a–d** *top*: (modified) BNC sample, *bottom left* negative control (paper disc), and *bottom right* positive control (amoxycillin/clavulanic acid)

Conclusion

We successfully demonstrated the preparation of hybrids consisting of BNC and AgNPs by utilizing a gentle synthesis route. The AgNPs grew selectively on the activated BNC surface. They were firmly immobilized on the cellulose fibers due to a chemical linkage to the grafted amine groups of the pre-modified BNC. Hence, the BNC-AgNP hybrids achieved extended lifetimes by avoiding the release of AgNPs. Furthermore, the amount of AgNPs on BNC was easily tunable by varying the concentration of $AgNO_3$ or the reaction time of BNC in the $AgNO_3$ solution. The hybrids exhibit a strong antimicrobial activity against *E. coli* even at low amounts of AgNPs. Altogether, due to the combination of the unique features of BNC for wound care and the antimicrobial properties of AgNPs, the produced hybrids are of potential interest for the application as antimicrobial dressings in wound care.

Acknowledgments The authors thank R. Zimmermann, INNOVENT e.V. Technologieentwicklung Jena, for his kind support during the antimicrobial studies and D. Reichmann for agar diffusion tests (Department of Dermatology and Allergology). F.W. acknowledges the DBU (Deutsche Bundesstiftung Umwelt) for financial support. C.W., D.K. and F.A.M. are grateful for the funding of this work by the Thuringian Ministry of Education, Science and Culture (B714-10032) and the European Fund for Regional Development.

References

Alila S, Ferraria AM, Botelho do Rego AM, Boufi S (2009) Controlled surface modification of cellulose fibers by amino derivatives using N N'-carbonyldiimidazole as activator. Carbohydr Polym 77(3):553–562. doi:10.1016/j.carbpol.2009.01.028

Arora A, Mitragotri S (2010) Novel topical microbicides through combinatorial strategies. Pharm Res 27(7): 1264–1272. doi:10.1007/s11095-010-0095-9

Barud HS, Regiani T, Marques RFC, Lustri WR, Messaddeq Y, Ribeiro SJL (2011) Antimicrobial bacterial cellulose—silver nanoparticles composite membranes. J Nanomat 2011:1–8. doi:10.1155/2011/721631

Bast E (2001) Mikrobiologische Methoden: Eine Einführung in grundlegende Arbeitstechniken, 2nd edn. Spektrum Akademischer Verlag GmbH, Heidelberg

Bhanat K, Parashar N, Jain K, Sharma VK (2011) Synthesis and antimicrobial study of 4-Benzylidene-2-phenyl-1-(5-phenylthiazole-2-yl)-1H-imidazol-5(4H)-one. Asian J Biochem Pharm Res 1(1):83–90

Boufi S, Ferraria AM, Botelho do Rego AM, Battaglini N, Herbst F, Rei Vilar M (2011) Surface functionalization of cellulose with noble metals nanoparticles through a selective nucleation. Carbohydr Polym 86(4):1586–1594. doi:10.1016/j.carbpol.2011.06.067

Bridges K, Kidson A, Lowbury EJL, Wilkins MS (1979) Gentamicin- and silver-resistant pseudomonas in a burns unit. Br Med J 1(6161):446–449. doi:10.1136/bmj.1.6161.446

Calfee DP (2012) Crisis in hospital-acquired, healthcare-associated infections. Annu Rev Med 63:359–371. doi:10.1146/annurev-med-081210-144458

Castellano JJ, Shafii SM, Ko F, Donate G, Wright TE, Mannari RJ, Payne WG, Smith DJ, Robson MC (2007) Comparative evaluation of silver-containing antimicrobial dressings and drugs. Int Wound J 4(2):114–122. doi:10.1111/j.1742-481X.2007.00358_2.x

Chawla A, Sharma A, Sharma AK (2012) A convenient approach for the synthesis of imidazole derivatives using microwaves. Chem Inform 43(24):116–140. doi:10.1002/chin.201224254

Cho K-H, Park J-E, Osaka T, Park S-G (2005) The study of antimicrobial activity and preservative effects of nanosilver ingredient. Electrochim Acta 51(5):956–960. doi:10.1016/j.electacta.2005.04.071

Chopra I (2007) The increasing use of silver-based products as antimicrobial agents: a useful development or a cause for concern? J Antimicrob Chemother 59(4):587–590. doi:10.1093/jac/dkm006

Czaja W, Krystynowicz A, Bielecki S, Brown RM Jr (2006) Microbial cellulose—the natural power to heal wounds. Biomaterials 27(2):145–151. doi:10.1016/j.biomaterials.2005.07.035

Czaja WK, Young DJ, Kawecki M, Brown RM Jr (2007) The future prospects of microbial cellulose in biomedical applications. Biomacromolecules 8(1):1–12. doi:10.1021/bm060620d

Ferraria AM, Boufi S, Battaglini N, Botelho do Rego AM, ReiVilar M (2010) Hybrid systems of silver nanoparticles generated on cellulose surfaces. Langmuir 26(3):1996–2001. doi:10.1021/la902477q

Fontana JD, De Souza AM, Fontana CK, Torriani IL, Moreschi JC, Gallotti BJ, De Souza SJ, Narcisco GP, Bichara JA, Farah LFX (1990) Acetobacter cellulose pellicle as a temporary skin substitute. Appl Biochem Biotechnol 24–25(1):253–264. doi:10.1007/BF02920250

Gallant-Behm CL, Yin HQ, Liu S, Heggers JP, Langford RE, Olson ME, Hart DA, Burrell RE (2005) Comparison of in vitro disc diffusion and time kill-kinetic assays for the evaluation of antimicrobial wound dressing efficacy. Wound Repair Regen 13(4):412–421. doi:10.1111/j.1067-1927.2005.130409.x

Gordon O, Slenters TV, Brunetto PS, Villaruz AE, Sturdevant DE, Otto M, Landmann R, Fromm KM (2010) Silver coordination polymers for prevention of implant infection: Thiol interaction, Impact on respiratory chain enzymes, and Hydroxyl Radical induction. Antimicrob Agents Chemother 54(10):4208–4218. doi:10.1128/AAC.01830-09

Heinze T, Liebert T, Heublein B, Hornig S (2006) Functional Polymers Based on Dextran. In: Klemm D (ed) Polysaccharides II Advances in Polymer Science, vol. 205, Springer, Heidelberg, pp 199–291. doi: 10.1007/12_100

Hestrin S, Schramm M (1954) Synthesis of cellulose by Acetobacter xylinum. 2. Preparation of freeze-dried cells capable of polymerizing glucose to cellulose. Biochem J 58(2):345–352

Hipler U-C, Elsner P, Fluhr JW (2006) Antifungal and antibacterial properties of a silver-loaded cellulosic fiber. J Biomed Mater Res B Appl Biomater 77B(1):156–163. doi:10.1002/jbm.b.30413

Ishida O, Kim D-Y, Kuga S, Nishiyama Y, Brown RM Jr (2004) Microfibrillar carbon from native cellulose. Cellulose 11(3–4): 475–480. doi:10.1023/B:CELL.0000046410.31007.0b

Jonas R, Farah LF (1998) Production and application of microbial cellulose. Polym Degrad Stab 59(1–3):101–106. doi:10.1016/S0141-3910(97)00197-3

Klemm D, Schumann D, Udhardt U, Marsch S (2001) Bacterial synthesized cellulose—artificial blood vessels for microsurgery. Prog Polym Sci 26(9):1561–1603. doi:10.1016/S0079-6700(01)00021-1

Klemm D, Heublein B, Fink H-P, Bohn A (2005) Cellulose: fascinating biopolymer and sustainable Raw material. Angew Chem Int Edit 44(22):3358–3393. doi:10.1002/anie.200460587

Klemm D, Schumann D, Kramer F, Heßler N, Hornung M, Schmauder H-P, Marsch S (2006) Nanocelluloses as innovative polymers in research and application. Adv Polym Sci 205(August):49–96. doi:10.1007/12_097

Klemm D, Kramer F, Moritz S, Lindström T, Ankerfors M, Gray D, Dorris A (2011) Nanocelluloses: a new family of nature-based materials. Angew Chem Int Edit 50(24):5438–5466. doi:10.1002/anie.201001273

Knetsch MLW, Koole LH (2011) New strategies in the development of antimicrobial coatings: the example of increasing usage of silver and silver nanoparticles. Polymers 3(1):340–366. doi:10.3390/polym3010340

Kralisch D, Hessler N, Klemm D, Erdmann R, Schmidt W (2010) White biotechnology for cellulose manufacturing—the HoLiR concept. Biotechnol Bioeng 105(4):740–747. doi:10.1002/bit.22579

Loh JV, Percival SL, Woods EJ, Williams NJ, Cochrane CA (2009) Silver resistance in MRSA isolated from wound and nasal sources in humans and animals. Int Wound J 6(1):32–38. doi:10.1111/j.1742-481X.2008.00563.x

Maneerung T, Tokura S, Rujiravanit R (2008) Impregnation of silver nanoparticles into bacterial cellulose for antimicrobial wound dressing. Carbohydr Polym 72(1):43–51. doi:10.1016/j.carbpol.2007.07.025

Monteiro DR, Gorup LF, Takamiya AS, Ruvollo-Filho AC, de Camargo ER, Barbosa DB (2009) The growing importance of materials that prevent microbial adhesion: antimicrobial effect of medical devices containing silver. Int J Antimicrob Agents 34(2):103–110. doi:10.1016/j.ijantimicag.2009.01.017

Morones JR, Elechiguerra JL, Camacho A, Holt K, Kouri JB, Ramírez JT, Yacaman MJ (2005) The bactericidal effect of silver nanoparticles. Nanotechnology 16(10):2346–2353. doi:10.1088/0957-4484/16/10/059

Panyala NR, Peña-Méndez EM, Havel J (2008) Silver or silver nanoparticles: a hazardous threat to the environment and human health? J Appl Biomed 6(3):117–129

Percival SL, Bowler PG, Russell D (2005) Bacterial resistance to silver in wound care. J Hosp Infect 60(1):1–7. doi:10.1016/j.jhin.2004.11.014

Rodríguez-Gattorno G, Díaz D, Rendón L, Hernández-Segura GO (2002) Metallic Nanoparticles from Spontaneous Reduction of Silver(I) in DMSO. Interaction between Nitric Oxide and Silver Nanoparticles. J Phys Chem B 106(10):2482–2487. doi:10.1021/jp012670c

Schierholz JM, Lucas LJ, Rump A, Pulverer G (1998) Efficacy of silver-coated medical devices. J Hosp Infect 40(1): 257–262. doi:10.1016/S0195-6701(98)90301-2

Silver S (2003) Bacterial silver resistance: molecular biology and uses and misuses of silver compounds. FEMS Microbiol Rev 27(2–3):341–353. doi:10.1016/S0168-6445(03)00047-0

Solway DR, Clark WA, Levinson DJ (2011) A parallel open-label trial to evaluate microbial cellulose wound dressing in the treatment of diabetic foot ulcers. Int Wound J 8(1):69–73. doi:10.1111/j.1742-481X.2010.00750.x

Sondi I, Salopek-Sondi B (2004) Silver nanoparticles as antimicrobial agent: a case study on *E. coli* as a model for Gram-negative bacteria. J Colloid Interface Sci 275(1): 177–182. doi:10.1016/j.jcis.2004.02.012

Sureshkumar M, Siswanto DY, Lee C-K (2010) Magnetic antimicrobial nanocomposite based on bacterial cellulose and silver nanoparticles. J Mater Chem 20(33):6948–6955. doi:10.1039/c0jm00565g

Walker M, Hobot JA, Newman GR, Bowler PG (2003) Scanning electron microscopic examination of bacterial immobilisation in a carboxymethyl cellulose (AQUACEL) and alginate dressings. Biomaterials 24(5):883–890

Waring MJ, Parsons D (2001) Physico-chemical characterization of carboxymethylated spun cellulose fibres. Biomaterials 22(9):903–912. doi:10.1016/S0142-9612(02)00414-3

Wesarg F, Schlott F, Grabow J, Kurland H-D, Heßler N, Kralisch D, Müller FA (2012) In situ synthesis of photocatalytically active hybrids consisting of bacterial nanocellulose and anatase nanoparticles. Langmuir 28(37):13518–13525. doi:10.1021/la302787z

Wiegand C, Elsner P, Hipler U-C, Klemm D (2006) Protease and ROS activities influenced by a composite of bacterial cellulose and collagen type I in vitro. Cellulose 13(6): 689–696. doi:10.1007/s10570-006-9073-0

Yang J, Yu J, Sun D, Yang X (2011) Preparation of novel Ag/bacterial cellulose hybrid nanofibers for antimicrobial wound dressing. Adv Mat Res 152-153:1771-1774. doi:10.4028/www.scientific.net/AMR.152-153.1771

Yang G, Xie J, Hong F, Cao Z, Yang X (2012) Antimicrobial activity of silver nanoparticle impregnated bacterial cellulose membrane: effect of fermentation carbon sources of bacterial cellulose. Carbohydr Polym 87(1):839–845. doi:10.1016/j.carbpol.2011.08.079

Yun YS, Bak H, Jin H-J (2010) Monolithic macroporous carbon cryogel prepared from natural polymers. J Korean Phys Soc 57(6):1950–1952. doi:10.3938/jkps.57.1950

Zimmermann R, Pfuch A, Horn K, Weisser J, Heft A, Röder M, Linke R, Schnabelrauch M, Schimanski A (2011) An approach to create silver containing antimicrobial coatings by use of atmospheric pressure plasma chemical vapour deposition (APCVD) and combustion chemical vapour deposition (CCVD) in an economic way. Plasma Process Polym 8(4):295–304. doi:10.1002/ppap.201000113